Journal of the Brazilian Society of Mechanical Sciences and Engineering (2020) 42:105
https://doi.org/10.1007/s40430-020-2185-x

TECHNICAL PAPER

A new skeletal mechanism for ethanol using a modified implementation methodology based on directed relation graph (DRG) technique

Felipe Minuzzi[1] · **Jean Monteiro de Pinho**[2,3]

Received: 26 November 2018 / Accepted: 11 January 2020 / Published online: 28 January 2020

Abstract
A different methodology for implementing the standard mechanism reduction technique directed relation graph (DRG) is presented and applied to develop a new skeletal mechanism for ethanol. Two combustion processes, ignition delay time and flame speed, that are mandatory for a mechanism to reproduce are used to calculate the species coupling through DRG index. Based on a detailed mechanism of 57 species among 383 reversible elementary reactions, a skeletal mechanism of 37 species and 184 reactions is obtained, which represents a decrease of 35% in the number of species and almost 52% in the number of reactions. The new mechanism is validated for ignition delay time and flame speed measurements, and also for one-dimensional burner stabilized flat and counterflow flames simulations, which were not considered in the development of the skeletal mechanism. Comparisons with experimental data and with the behaviour of other mechanisms in the literature are also displayed. The methodology presented can be useful and contribute to generate skeletal mechanisms with less effort that can reproduce a more demanding simulation.

Keywords Chemical modelling · Ethanol · Skeletal mechanism · Combustion · DRG

1 Introduction

Energy conversion is a fundamental resource of today's society well-being. In 2017, world consumption of energy was approximately 13511.2 Mtoe (million tonnes oil equivalent), of which 34% was derived from oil, 23% from natural gas, 27% from coal and, in this scenario, only 3% is related with renewable energy sources [3]. Most of the consumed energy worldwide is due to fossil fuels, a process that generates several gaseous and particulate emissions which are harmful to human health and motivates environmental imbalance. Despite the growth in using renewable energy, combustion will remain being the major source of conversion for several years [30]. Nonetheless, the fuel to be burned will be different, and considerable studies are being focused in the use of biofuels, such as ethanol and biodiesel.

Among biofuels, the use of ethanol (C_2H_5OH) as an energy source that can be produced through renewable resources stands out. Most of this fuel is derived from the fermentation of sugar cane, although studies show that it can also be derived from other types of biomass, such as raw material of cellulose, corn stalk, rice straw, beet, wood pulp and municipal solid waste.

Therefore, it is natural that studies regarding the oxidation of ethanol emerge. In the past years, several studies were developed in order to study the kinetics and the combustion characteristics of ethanol [5–7, 13, 21–23, 27, 31]. Egolfopoulos et al. [8] did an experimental and numerical study on ethanol oxidation kinetics, using counterflow premixed flame to determine laminar flame speed, flow and shock tube reactors. Ignition of ethanol in a shock tube reactor was studied both numerically and experimentally by Curran et al. [4]. Marinov [20] proposed a detailed kinetic mechanism for

Technical Editor: Fernando Marcelo Pereira, Ph.D.

✉ Felipe Minuzzi
felipe.minuzzi@ufrgs.br

[1] Reactive Fluid Mechanics Group, National Institute for Space Research - INPE, Rod. Presidente Dutra, km 40, 12630-000 Cachoeira Paulista, SP, Brazil

[2] Graduate Program in Chemical Engineering, Federal University of Rio Grande do Sul, Engenheiro Luiz Englert St, Building, 12204 Porto Alegre, RS, Brazil

[3] Federal Institute of Santa Catarina, Euclides Hack St, 1603 Xanxerê, SC, Brazil

ethanol oxidation in high temperatures. The validation was performed with simulations of constant volume bomb and counterflow flames for laminar flame speed, shock wave to catch ignition delay time and ethanol oxidation product profiles from jet-stirred and turbulent flow reactor. Saxena and Williams [32] proposed a detailed kinetic mechanism for ethanol oxidation and developed numerical and experimental studies to validate it. The concentration of pollutants was also investigated. Nevertheless, these works are focused in a diverse range of parameters and applications, and usually are only applicable to the conditions in which they were validated.

Recently, Olm et al. [28], in an attempt to overcome this problem, developed and detailed mechanism that is suitable to cover a wide range of parameters and applications, using an optimization approach and based on an modified version of the mechanism developed by Saxena and Williams [32]. The validation was held out for a great amount of available experimental data, and the authors claim that the mechanism provides the best description of the currently available experimental data.

However, using detailed kinetic mechanisms in the simulation is computationally prohibitive. Techniques for chemical reduction are mandatory in order to develop reduced models with less variables and moderate stiffness, so that for a specific application and interval of operating conditions, accuracy can be maintained. The purpose of techniques for chemical reduction is to limit the number of intermediary species and reduce the number of equations to be solved in order to represent with accuracy the behaviour of the main species [37]. A complete review of the chemical reduction techniques can be found in the works of Goussis and Maas [11], Griffiths [12], Løvås [15] and Tomlin et al. [34].

The directed relation graph (DRG), developed by Lu and Law in 2005 [16, 17], is a reduction method based on the construction of skeletal mechanisms, and consists in evaluating the error produced when one species is withdraw of the full mechanism. For its implementation, different applications must be defined so that the resulting skeletal mechanism can reproduce with accuracy different combustion processes. Usually, DRG is a first stage step to produce a reduced mechanism, and can be used to reduce very large fuels mechanisms [1, 14, 19, 24, 26, 33, 39]

In the present work, a new skeletal mechanism for ethanol oxidation is developed using DRG. Compared to the original DRG formulation [16], we propose a slightly different implementation methodology. Two applications, namely, ignition delay time and flame speed are considered to generate a skeletal mechanism that can be used in different combustion processes. Results are validated for ignition delay times, premixed flat and counterflow diffusion flames for different equivalence ratios, so rich, lean and stoichiometric mixtures can be analysed.

2 Chemical reduction: directed relation graph

The modelling of chemical kinetics must consider the accurate description of concentrations profiles of the important species that can be defined according to the objective of the model [36]. For such purpose, necessary species should remain in the model, so that the important characteristics of the important species are well-described. All other species can be considered redundant, and thus withdraw of the resulting skeletal mechanism. Subsequently, reactions that contribute little to the remaining species are eliminated.

The methods for skeletal reduction can be applied locally, i.e. for specific pressure, temperature and concentration profiles. In this case, the achievement of a good skeletal scheme for a more complex combustion situation depends on the range of conditions to give the reduced model validity in reproducing certain features.

An important consideration to be made is that since most methods depends on the concentration of the species through a specific application, the process should be repeated to different configurations, i.e. several states over the trajectory of a species. The ones that are considered redundant to all relevant simulations and conditions are removed from the mechanism.

The directed relation graph (DRG), developed by [16], is a reduction method based on the construction of skeletal mechanisms. The aim of the method is to efficiently solve the species coupling, so that those who has little or no influence on the important species can be removed.

The contribution of species B in the production/consumption rate of species A can be quantified through the normalized index r_{AB}, given by

$$r_{AB} = \frac{\sum_{i=1}^{n_r} \left| \nu_{A,i} \dot{\omega}_i \delta_{B,i} \right|}{\sum_{i=1}^{n_r} \left| \nu_{A,i} \dot{\omega}_i \right|}, \tag{1}$$

where $\nu_{A,i}$ is the stoichiometric coefficient of A in reaction i, $\dot{\omega}_i$ is the reaction rate, n_r the number of reactions and $\delta_{B,i}$ is

$$\delta_{B,i} = \begin{cases} 1, & \text{if the } i\text{th elementary reaction involves species B;} \\ 0, & \text{otherwise.} \end{cases} \tag{2}$$

The terms in the denominator of Eq. (1) are the contribution of reactions to the production/consumption of species A, and the terms in the numerator are those from the denominator that involve species B [17].

Defining a threshold limit value ϵ ($0 < \epsilon < 1$), and if index r_{AB} is bigger compared to this threshold ($r_{AB} > \epsilon$), then removing species B can induce error in the production of species A, so that species B must be maintained in the skeletal mechanism. Usually, species A are chosen as those who

have some desirable chemical attributes that the reduced mechanism should reproduce [29], and called target species.

The specification of target species is arbitrary and decided considering the range of parameters and application. A combination of fuel molecules, oxygen and main products of combustion is an appropriate starting set [35, 40]. Recent works developed an automated strategy to deal with this issue, where the target species is dynamic and automatically identified through a simplified algorithm [2, 9].

The resulting skeletal mechanism obtained has errors according to the user-specified threshold ϵ for the conditions under which it is developed [16]. Therefore, mechanisms with different levels of accuracy can be obtained by assigning different values for ϵ. The skeletal mechanism will converge in detail as ϵ is approaching zero, and the number of species can vary abruptly as the threshold is varied.

To obtain a mechanism over a sufficiently wide range of parameters, such as pressure, temperature, equivalence ratio and resident time, a group of points in the parametric space are sampled for typical applications [17]. Consequently, for each application, a skeletal sub-mechanism can be obtained for each point considered, and the union of these consists of the application-specific skeletal mechanism. Finally, the union of those generates an efficient skeletal mechanism that can describe the applications for which was developed over all the parameters.

3 Methodology for implementing DRG

The DRG computational code was implemented in Python, using the open-source software Cantera [10] for the zero- and one-dimensional simulations. Cantera is an open-source object-oriented software for problems involving chemical kinetics, thermodynamics and transport processes. The choice for Cantera was due the free availability to obtain it, as well as its easy usage and the possibility of using functions that facilitate the implementation of DRG.

The proposed methodology differs from the original strategy based on implementation. The original DRG [16, 17] aims to construct the graph whose edges are species, calculate the weights of each coupling and define dependent sets for each species, using for this a depth first search (DFS) algorithm (or, e.g. the Dijkstra algorithm [25]). However, in this work, the methodology (explained below) is based on the numerical simulations of combustion processes, using the concentrations profiles and temperature from these simulations and, with that, defines which paths of reactions are important to represent the chosen applications and remain in the mechanism. The reactions are selected if they have the species in which index (1) is greater than the user-specified ϵ. Therefore, index (1) is used as a measure of importance of each species in the detailed mechanism against the target species.

The goal of this work is to apply the DRG for ethanol (C_2H_5OH). The detailed mechanism chosen was developed by [20], and consists of 57 species among 383 reversible elementary reactions. This mechanism was validated using experimental data from shock tube reactor and flame speed measurements. The applications that will be applied are a batch reactor, with constant volume and internal energy, aiming to catch the ignition delay time, and a freely propagating premixed flat flame, to catch the flame speed. The first is used to cover the range of low temperatures considering only the reaction progress, without any transport process, while the latter covers a one-dimensional flame with both reaction and transport (convection and diffusion). We show that even without taking into consideration a non-premixed flame, the skeletal mechanism generated reproduce with accuracy this type of flame. These situations will be calculated varying initial temperature, pressure and equivalence ratio.

Firstly, the targets species for the DRG was chosen, consisting of the fuel, oxygen and the main products of combustion, CO_2 and H_2O. These are the usual targets species when applying DRG [25, 26, 29]. However, it was observed that some species that was important to maintain the path of oxidation from fuel to products was not being retained by DRG, even for small ϵ. It is the case of C_2H_6 and CH_3CO. Also, C_2H_4, which appears to be produced only in one reaction, so its index will also be very small, was defined as a target species, since its presence is observed to be very important to maintain accuracy. Thus, the final set of target species used for DRG is: C_2H_5OH, O_2, CO_2, H_2O, C_2H_6, CH_3CO and C_2H_4. These species will play the role of A species in index (1), while the B species are all species of the detailed mechanism. The threshold value used was $\epsilon = 0.08$. This value was achieved for a simple DRG calculation for stoichiometric mixture in the ideal gas reactor, and is consistent with the values used in the literature [40]. Generally, a choice above 0.2 causes the eliminations of important species and those that are strongly coupled would be removed together from the mechanism [18]. This is shown in Fig. 1, which presents the number of species that are retained in the skeletal mechanism as the threshold ϵ increases. From 0.05 to 0.15, most of redundant species are withdraw. After this point, we have some constant values for the number of species or jumps of the strongly coupled groups. The used value of $\epsilon = 0.08$ is between the desirable range, and the accuracy of the mechanism is maintained.

The calculation is performed as follows: the detailed mechanism is used to simulate a freely propagating premixed flat flame in order to find the flame speed. Then, the DRG is applied using the species concentrations and temperature from these flat flame calculations. The species

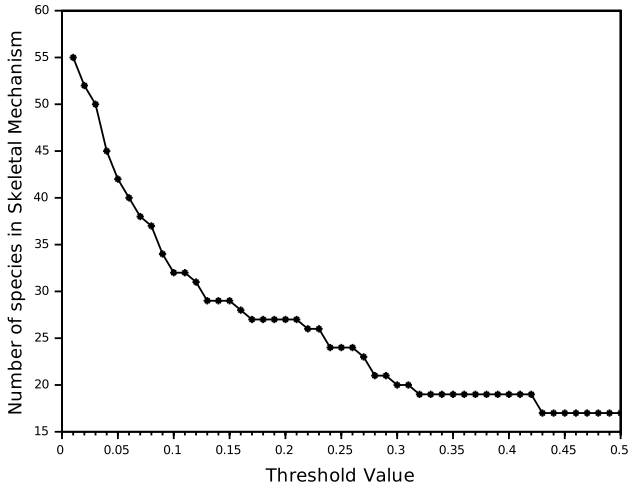

Fig. 1 Number of species retained in the skeletal mechanism against the threshold value ϵ

that has its index greater than the threshold is retained in a set; the others are discarded. The next step is to use the detailed mechanism to simulate an ideal gas reactor to catch the ignition time. Again, for each time step, the DRG is applied using concentrations and temperature from the reactor calculations, and the species with the index greater than the threshold are retained. Finally, the final set of species is found by the union of each application species set. The reactions containing only those species then are selected to be in the skeletal mechanism. The search stops at the first level, i.e. the DRG loop is not applied again to the final set of reactions. It is important to emphasize that the flat flame simulation is performed varying equivalence ratio from 0.5 to 2.0, while the pressure and temperature are varied from 1 atm to 100 atm and 500 K to 2000 K, respectively, in the reactor. For each of these parameters and each point in the domain of the simulation, the DRG is applied.

The skeletal mechanism obtained consists in 37 species and 184 reactions, which represents a decrease of 35% in the number of species and almost 52% in the number of reactions. This reduction is satisfactory since the remaining variables reproduce the detailed mechanism with accuracy. Error in flame speed and ignition time is less than 20% for all range of parameters. The skeletal mechanism is shown in the supplementary material, and its validation is shown in the next section.

4 Results and discussion

This section presents the numerical simulations for validating the skeletal mechanism developed with DRG. The simulations of this section were all carried out with Cantera [10]

Table 1 Number of species and reactions of different kinetic mechanism for the oxidation of ethanol

Mechanism	Number of species	Number of reactions	References
Marinov	57	383	[20]
Saxena and Williams	46	235	[32]
Olm et al.	49	251	[28]
Mittal et al.	113	710	[23]
Metcalfe et al.	253	1542	[21]
UC San Diego	50	247	[38]

The results are validated against available experimental data. To further show the efficiency of the proposed skeletal mechanism, the one-dimensional simulations of premixed and counterflow flames comparisons are also made with other mechanisms, which differ from size and range of parameters or applications: the already mentioned mechanisms of [20, 28, 32], and the mechanisms proposed by [21, 23, 38]. Characteristics of these mechanisms are shown in Table 1. To better show the results of the skeletal mechanism, these comparisons are made only for temperature and a few species mass fractions profiles.

4.1 Ignition delay times

The batch reactor is used to catch the autoignition time of the mixture. With Cantera, a reactor can be viewed as a box reduced to a single point, such that there is no spatial evolution but only temporal evolution of the quantities it contains. Thus, the evolution in time is carried out with a network of reactors, i.e. multiple reactors are interconnected, and the mass and heat flow among them are realized.

The autoignition time is calculated as the point where there is an exponential growth of OH radical, and the simulations are calculated varying the equivalence ratio ($\phi = 0.5, 1.0, 1.5, 2.0$) and pressure ($p = 1, 10, 35, 100$ atm). Simulations were performed for 800–2000 K temperature range. The same configuration is applied to the detailed and skeletal mechanism. The results are shown in Fig. 2 for different pressures and equivalence ratios.

Results show that the skeletal mechanism predicts very well the detailed model. This is expected, since the DRG was used using ignition as an application. Errors are below 10%. There is a small deviance from reduced and detailed model in high temperatures and pressure equal to 100 atm for the stoichiometric mixture. Nevertheless, these differences from reality are expected.

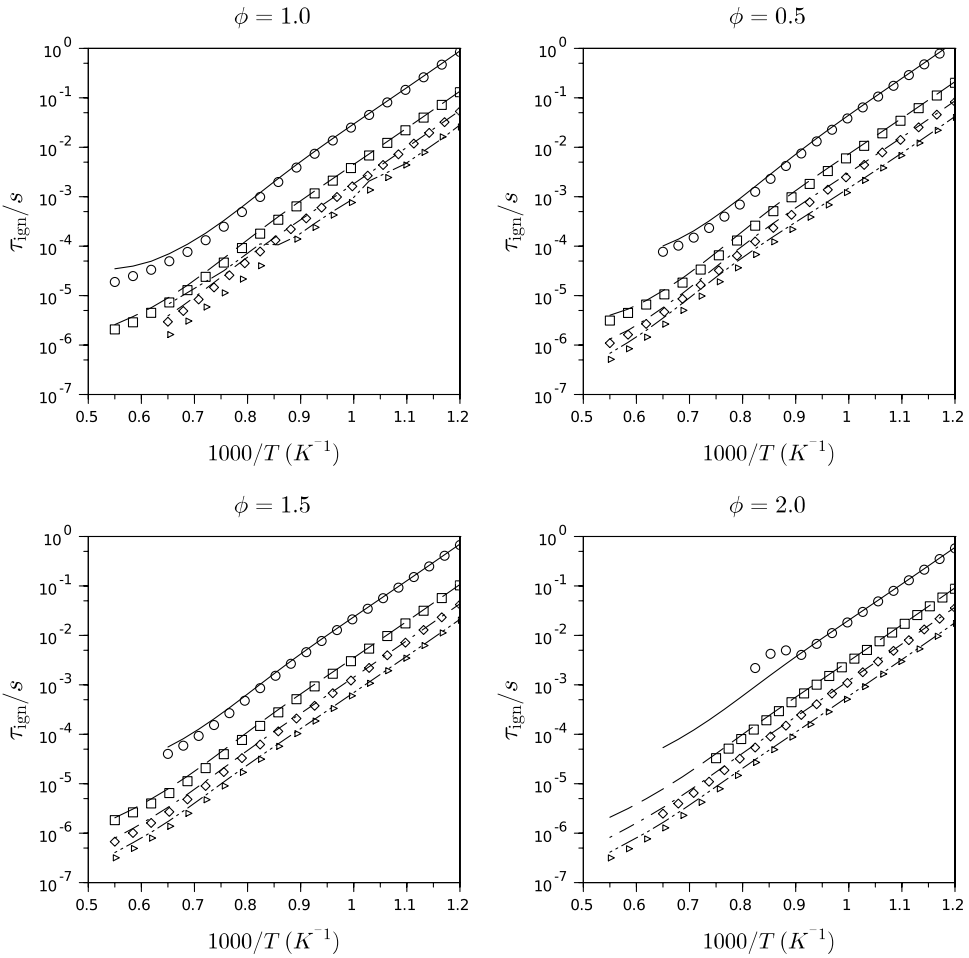

Fig. 2 Ignition delay times (s) for different pressures and equivalence ratios. Symbols are results for the detailed mechanisms [20]—circles: 1 atm; squares: 10 atm; diamonds: 35 atm and triangle: 100 atm—and lines for the skeletal mechanism

4.2 Premixed flames

The solution of a freely propagation premixed flat flame with Cantera follows the axisymmetric stagnation flow equations. The goal is to calculate the laminar flame speed for different values of equivalence ratio. We set different initial temperatures and maintain atmospheric pressure.

Figure 3 shows the comparison of the results between measurements and numerical simulations with the skeletal mechanism and the detailed mechanism of [20] for laminar flame speed calculated with the flat flame, for different initial temperatures. Experimental data are obtained from [8].

It can be seen that the lean zone of the flame shows practically the same behaviour as the experiment and other mechanism, and the region between $0.8 < \phi < 1.4$ presents the higher deviations. This is normal since several intermediate reactions were withdraw of the mechanism, which influences in the calculated laminar flame speed and depends of the activation energy. Besides, the skeletal mechanism reproduces the detailed mechanism, which has the same behaviour in this region. The deviations do not influence the validity of the model, since in most practice applications, combustion processes occur in lean-stoichiometric configurations.

Figures 4, 5, 6, 7, 8 and 9 show the results of a burner-stabilized flat flame, with a mixture of ethanol/air/argon, for three equivalence ratios ($\phi = 0.75, 1.0, 1.25$). These comparisons show the validity of the skeletal mechanism for low pressures, since the simulations were performed for 50mbar. The experimental data are from [13]. The burner consists of a cooled, brass, sintered plate, with 8cm diameter, in a vacuum chamber. The sampling position of the flame was varied by moving the burner to modify the distance of the quartz cone, and this was adjusted for the comparisons in this work. The conditions used are shown in Table 2, the same used in [13].

Figures 4, 5 and 6 show the comparison between the skeletal mechanism with other mechanisms and the experimental data, for temperature and mole fraction of fuel. It can observe a good agreement for the skeletal mechanism for these quantities, specially with other mechanisms. The peak for temperature for the stoichiometric flame in the experiment is $T = 1820$, while for the skeletal mechanism is $T = 1825$. In the lean flame, peaks are $T = 1752$

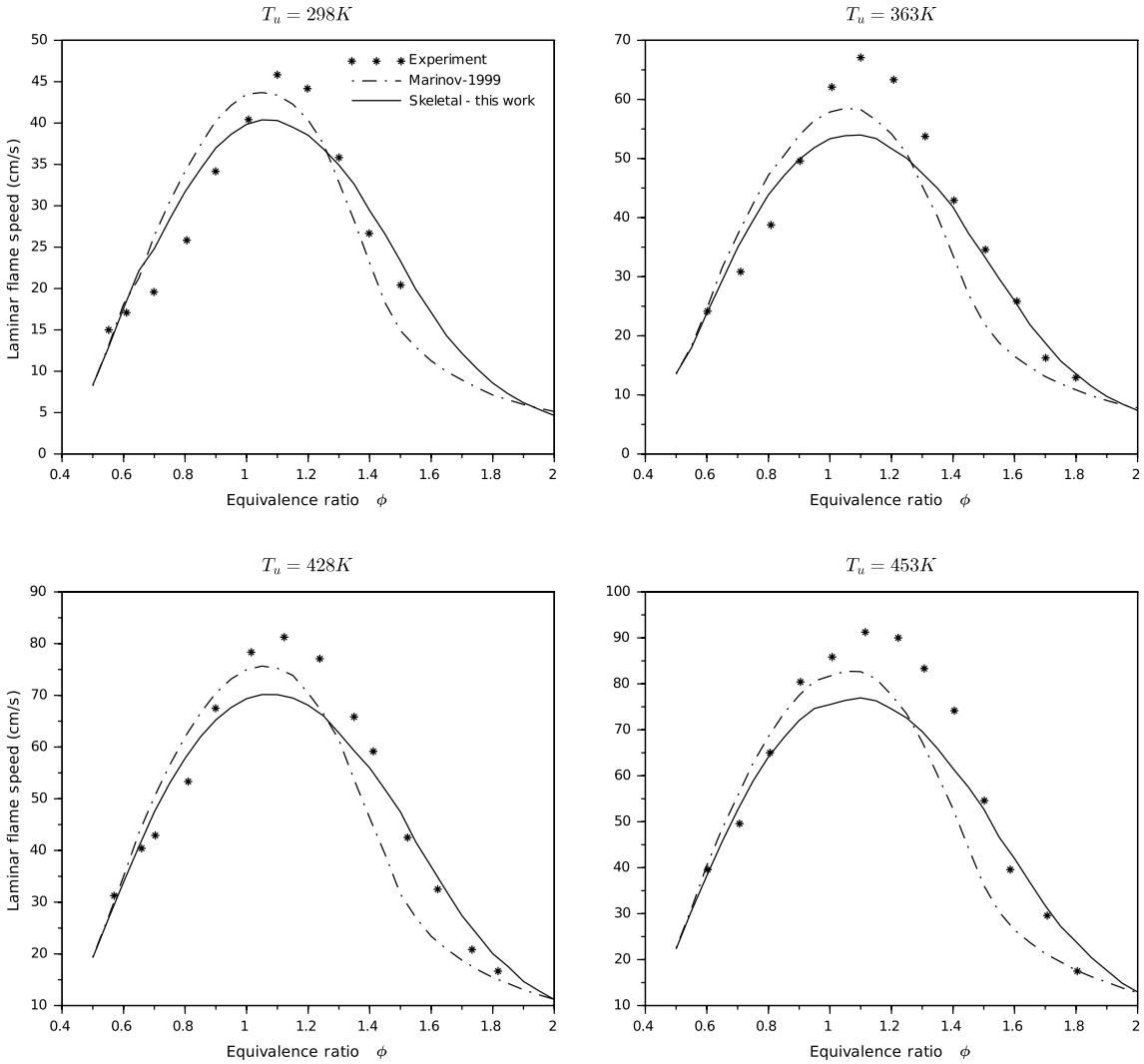

Fig. 3 Laminar flame speed calculated in a freely propagating flat flame for ethanol for different initial temperatures. The result of the skeletal mechanism is compared with different mechanisms in the literature and experimental data [8]

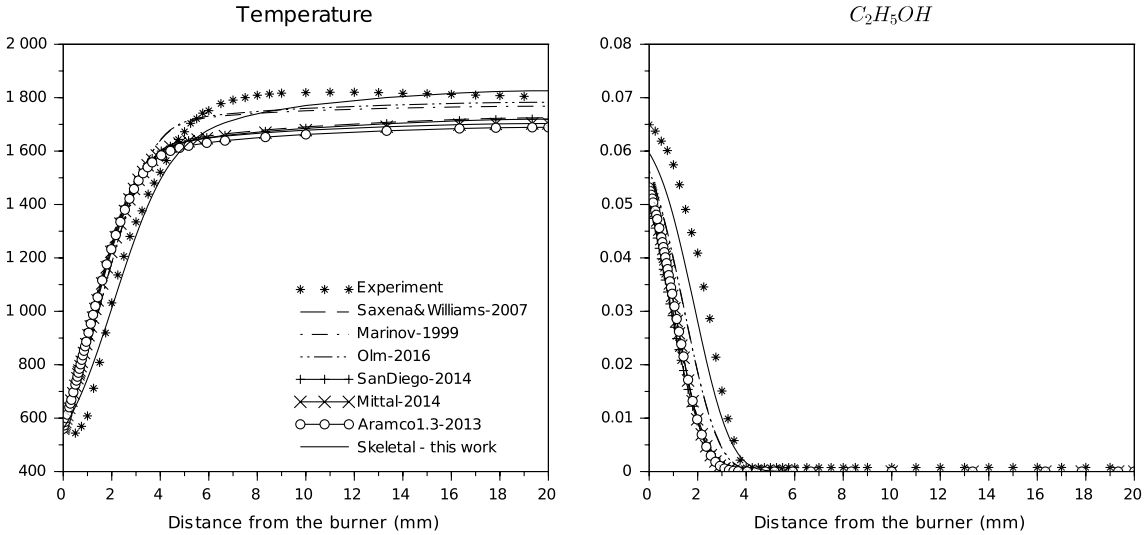

Fig. 4 Temperature and fuel mole fraction for different mechanisms against experimental data from [13] at $\phi = 1.0$. Results are for a burner-stabilized flat flame with initial temperature $T_u = 560$ K and atmospheric pressure

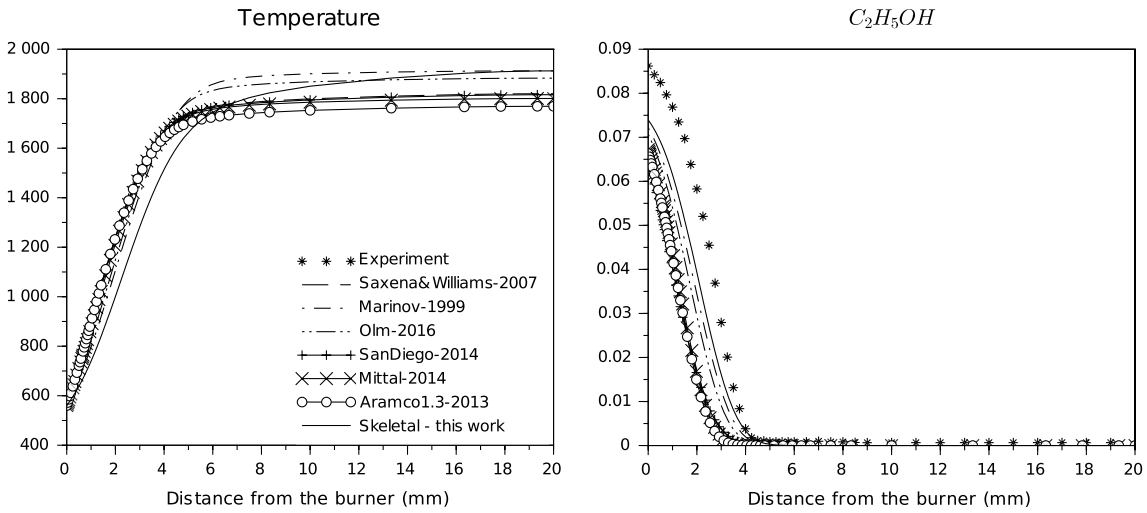

Fig. 5 Temperature and fuel mole fraction for different mechanisms against experimental data from [13] at $\phi = 1.25$. Results are for a burner-stabilized flat flame with initial temperature $T_u = 560$ K and atmospheric pressure

and $T = 1702$ and in the rich, $T = 1740$ and $T = 1912$, for experiment and skeletal mechanism, respectively.

Figures 7, 5 and 9 show the comparison of main species and radicals mole fractions between skeletal, detailed and experimental data. The lean flame shows the higher deviance when compared to the experimental data, with a under-prediction in almost all quantities, although the same behaviour of the skeletal is observed for the detailed mechanism. Besides, the low pressure used in these simulations is not in the range used for developing the skeletal mechanism, which can explain the deviations. Nevertheless, the results present the expected performance to reproduce a burner flat flame, although this was not the same used in developing the skeletal mechanism.

4.3 Counterflow flames

Albeit counterflow flames are not used in DRG as an application; it consists of one of the best simulations to validate a reduced model, since this type of flame has a very evident diffusion process. Besides that, a good result from counterflow simulations can indicate that the skeletal mechanism will provide good and reliable result for two- or three-dimensional CFD simulations, specially turbulent flows. We choose not to consider this type of flame when generating

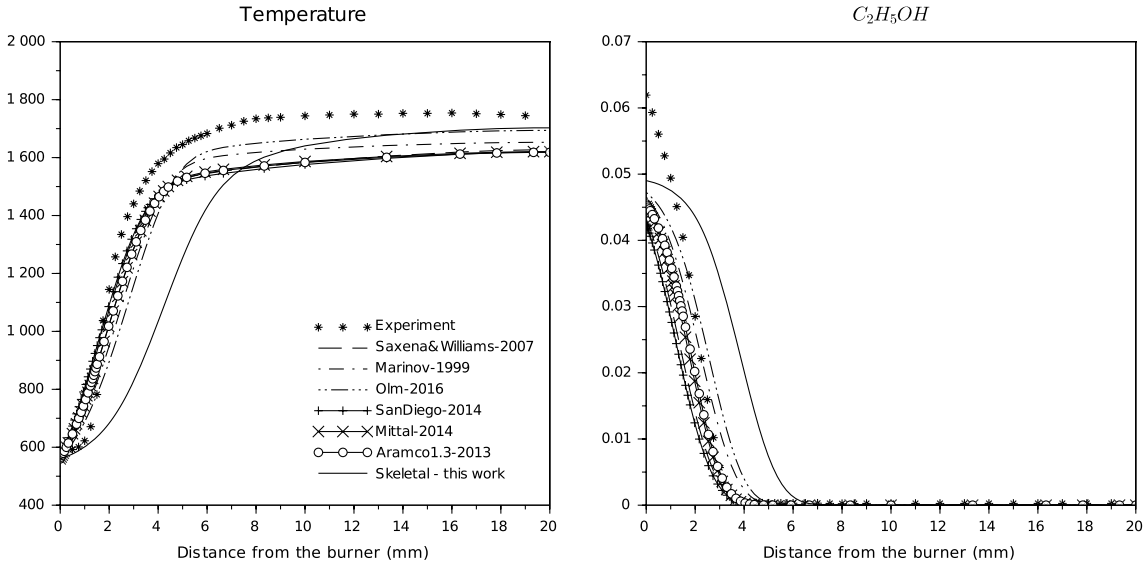

Fig. 6 Temperature and fuel mole fraction for different mechanisms against experimental data from [13] at $\phi = 0.75$. Results are for a burner stabilized flat flame with initial temperature $T_u = 560$ K and atmospheric pressure

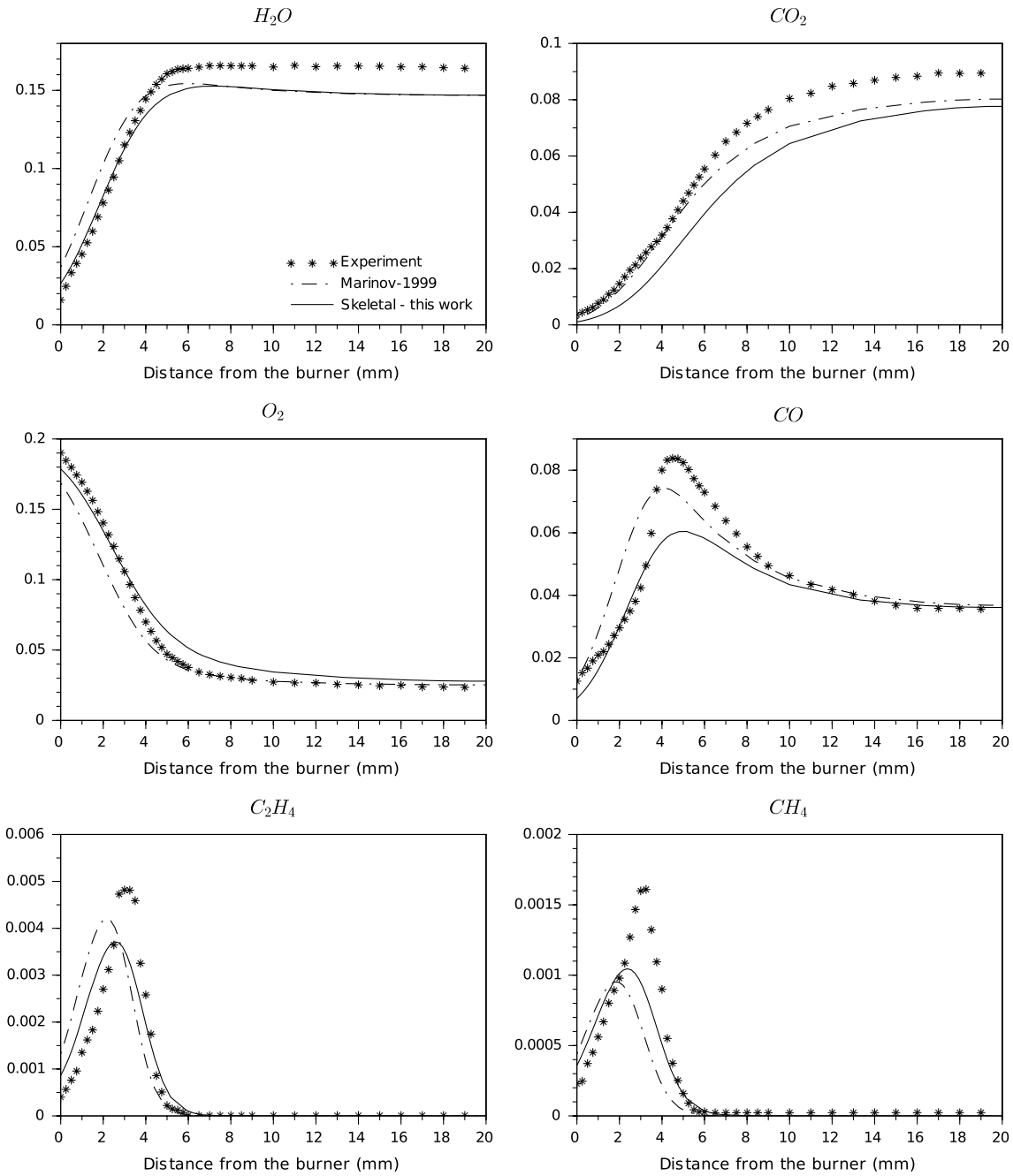

Fig. 7 Species mole fractions for detailed and skeletal mechanisms against experiment data from [13] at $\phi = 1.0$. Results are for a burner-stabilized flat flame with initial temperature $T_u = 560$ K and atmospheric pressure

the skeletal mechanism because it would largely increase the computational time of the reduction process.

The boundary conditions to calculate the counterflow flames are displayed in Table 3 for both streams and configurations. Those are the same values of the experiment carried out by [32].

The experimental counterflow burner [32] consists of two opposing ducts of 23.1mm inner diameter with shielding of annular nitrogen curtains separated by 12mm. Air flows from the top duct and fuel through the bottom duct at flow rates adjusted according to a momentum balance to maintain the stagnation plane halfway between the duct exits. An insulated vaporizer, temperature controlled to provide the desired ethanol mole fraction in nitrogen, generates the fuel vapour which flows through a heated line to the lower duct.

Figures 10, 11, 12 and 13 show the results for counterflow flames of both premixed and non-premixed ethanol/air

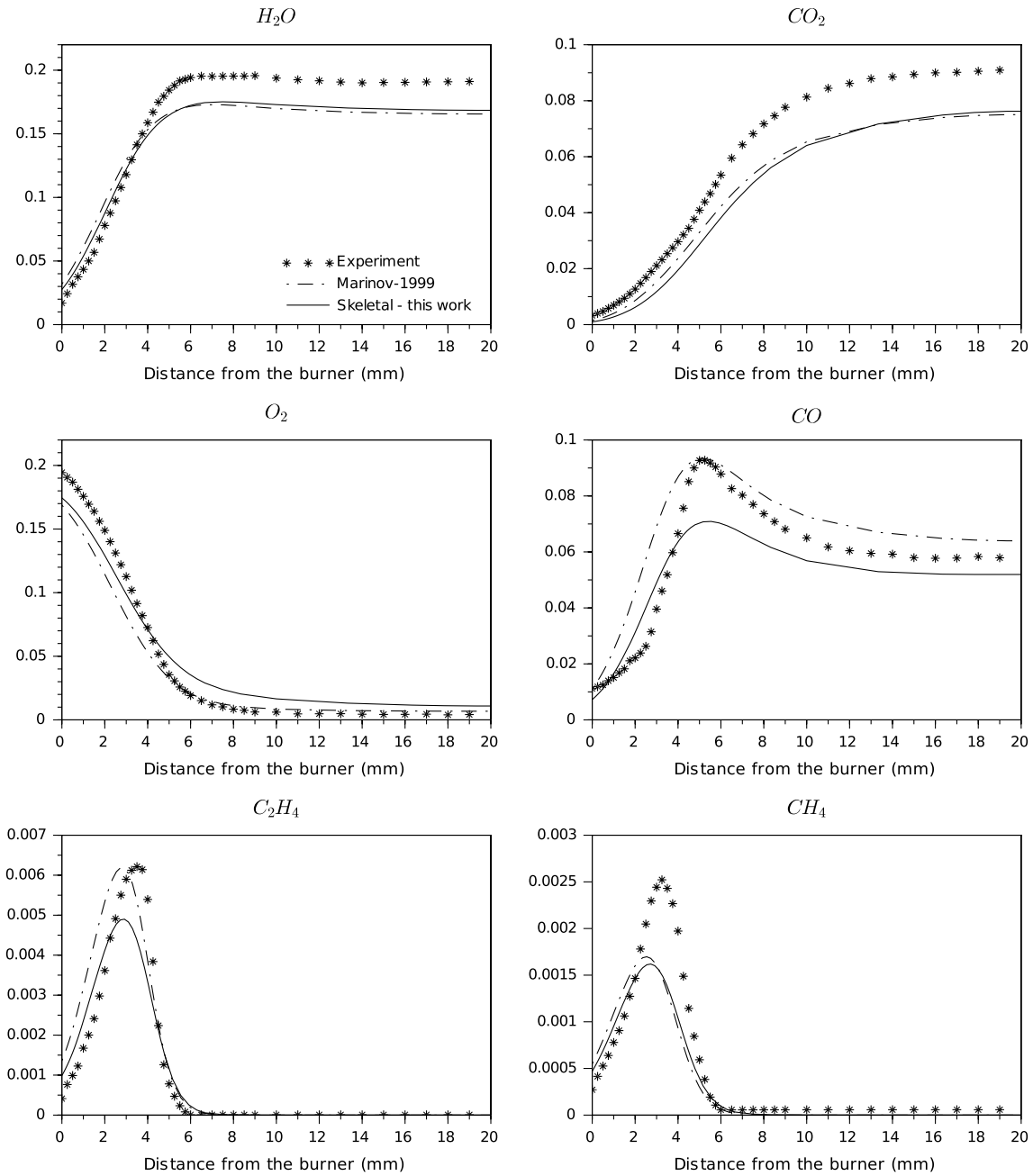

Fig. 8 Species mole fractions for detailed and skeletal mechanisms against experiment data from [13] at $\phi = 1.25$. Results are for a burner-stabilized flat flame with initial temperature $T_u = 560\,\mathrm{K}$ and atmospheric pressure

mixture. The temperature and mass fractions of fuel, oxidizer ad nitrogen are compared with experiment and different mechanisms (Figs. 10 and 11), while main species are compared between experimental, detailed and experiment (Figs. 12 and 13).

In the non-premixed flame, the results of the skeletal mechanism reproduce exactly the detail for the principal reactants and products. Over-prediction can be observed for H_2O and under-prediction occurs for CO and H_2. The skeletal mechanism also has results that are consistent with other mechanisms. The adiabatic maximum temperature achieved by the skeletal mechanism is $T = 1637\,\mathrm{K}$, while the detail results in $T = 1740\,\mathrm{K}$ and the experimental value is $T = 1811\,\mathrm{K}$. Despite that, the results of the reduced model shows that it can be used in other simulations, validating that the results will remain in an acceptable error range.

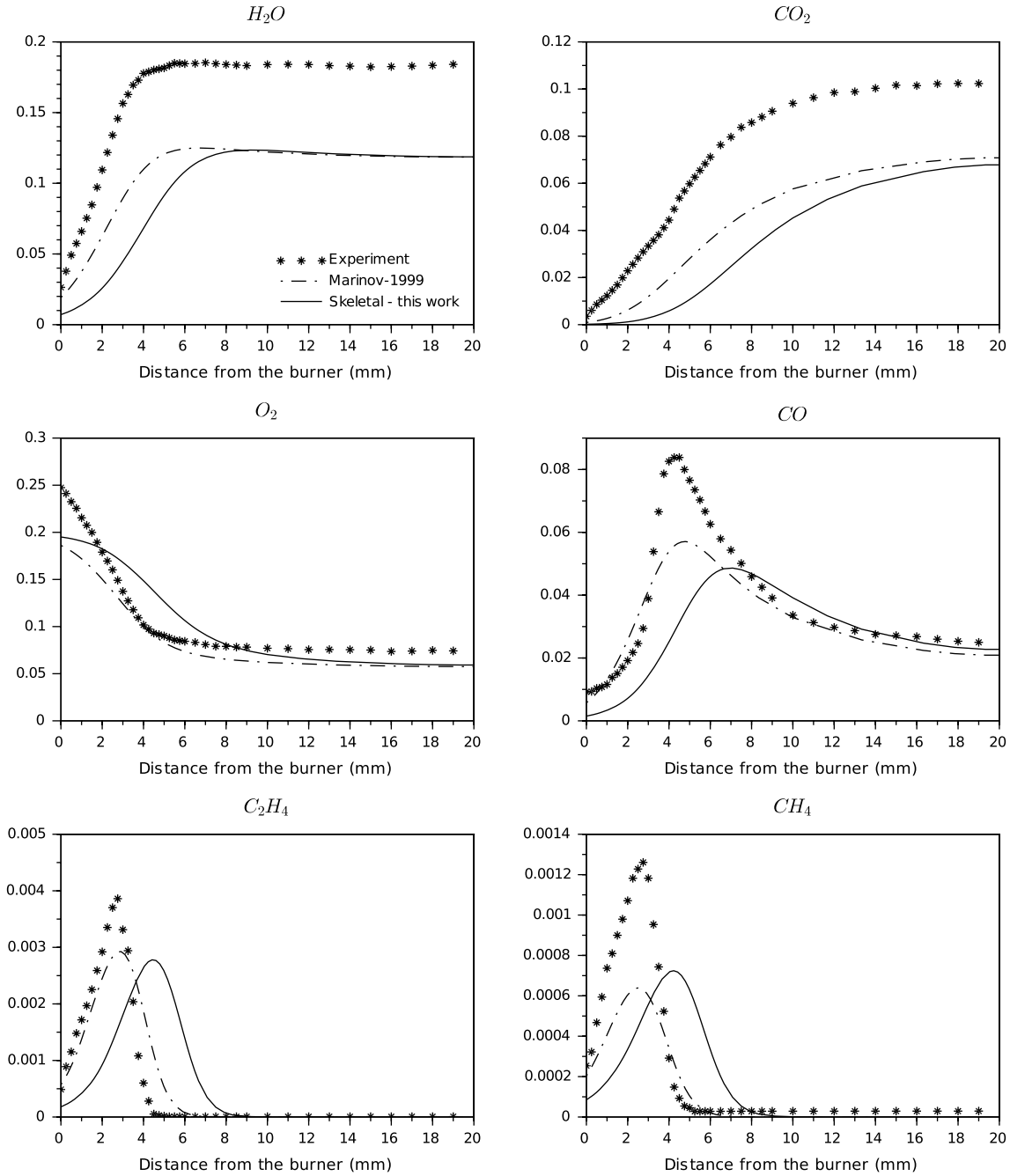

Fig. 9 Species mole fractions for detailed and skeletal mechanisms against experiment data from [13] at $\phi = 0.75$. Results are for a burner-stabilized flat flame with initial temperature $T_u = 560$ K and atmospheric pressure

Table 2 Flame conditions for the burner-stabilized flat flame (species in mole fractions)

Equiv. ratio (ϕ)	C_2H_5OH	O_2	Ar
1.00	0.069	0.206	0.725
0.75	0.069	0.275	0.657
1.25	0.085	0.206	0.709

Comparisons for a premixed counterflow flame show almost the same results that are observed from the non-premixed flames, with over-prediction for H_2O, and under-prediction for CO and H_2. However, the temperature profile shows exactly the same values for detailed and skeletal mechanism, with a peek in $T = 1990$ K and $T = 1991$ K, respectively. The experiment yields $T = 2151$ K.

Table 3 Conditions used in the simulation of a non-premixed counterflow flames

	Non-premixed flame		Premixed flame	
	Fuel stream	Ox. stream	Fuel stream	Ox. stream
$X_{C_2H_5OH}$	0.3	0	0.1385	0
X_{N_2}	0.7	0.79	0.6803	0.79
X_{O_2}	0	0.21	0.1812	0.21
Velocity (cm/s)	29.8	30	30.22	30
Temperature (K)	340	298	327	298
Pressure (atm)	1	1	1	1

Species quantities are given in mole fractions

Results for both calculations, premixed and non-premixed, of counterflow flames show that the skeletal mechanism can reproduce with accuracy the existing diffusion processes in reactive flow simulations. One difference that can be seen in the figures is that premixed flames produce higher quantities of CO, while the quantities for CO_2 are practically the same. This can be explained since there is a higher amount of oxygen in the fuel side of the burner, which also makes the production of CO to start sooner in the domain. The presence of oxygen also explains why the fuel is consumed earlier in premixed flames, which influence the mass fraction of H_2, that is almost two times the value for non-premixed.

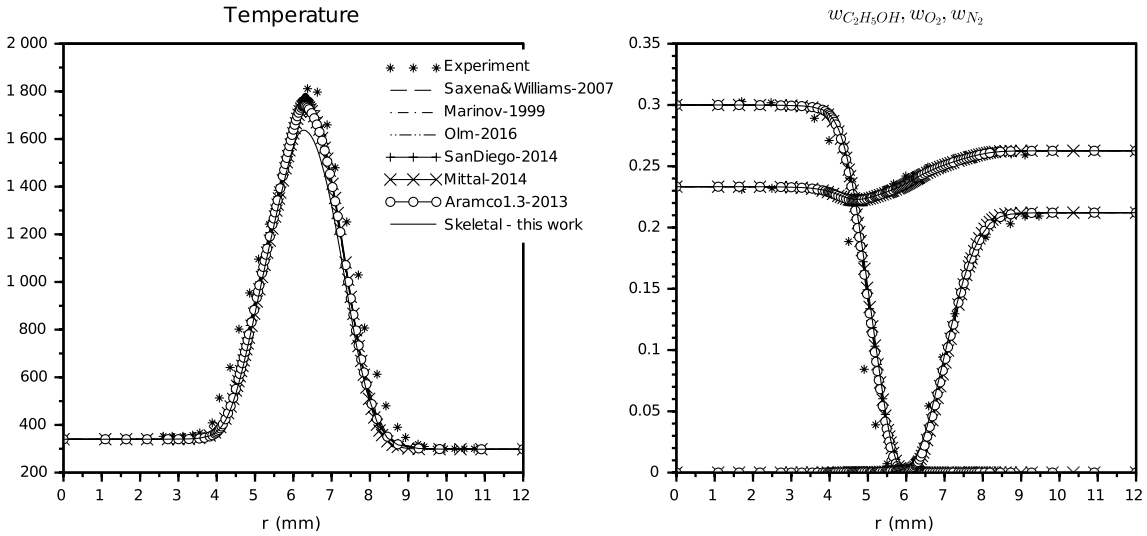

Fig. 10 Temperature and species mass fractions of fuel, oxidizer and nitrogen for different mechanisms for a non-premixed counterflow flame, compared with measurements [32]. The boundary conditions are given in Table 3

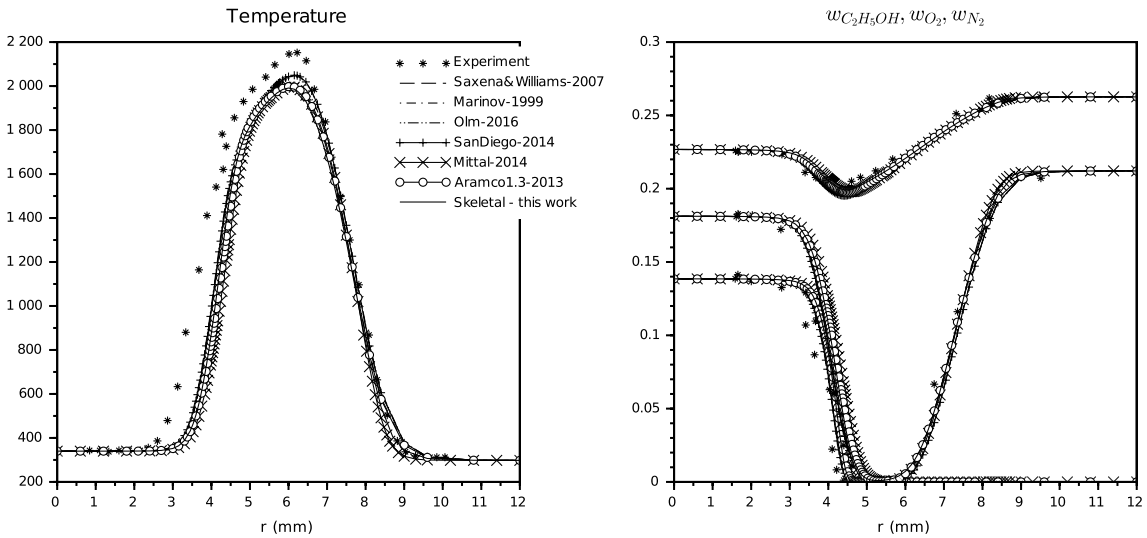

Fig. 11 Temperature and species mass fractions of fuel, oxidizer and nitrogen for different mechanisms for a premixed counterflow flame, compared with measurements [32]. The boundary conditions are given in Table 3

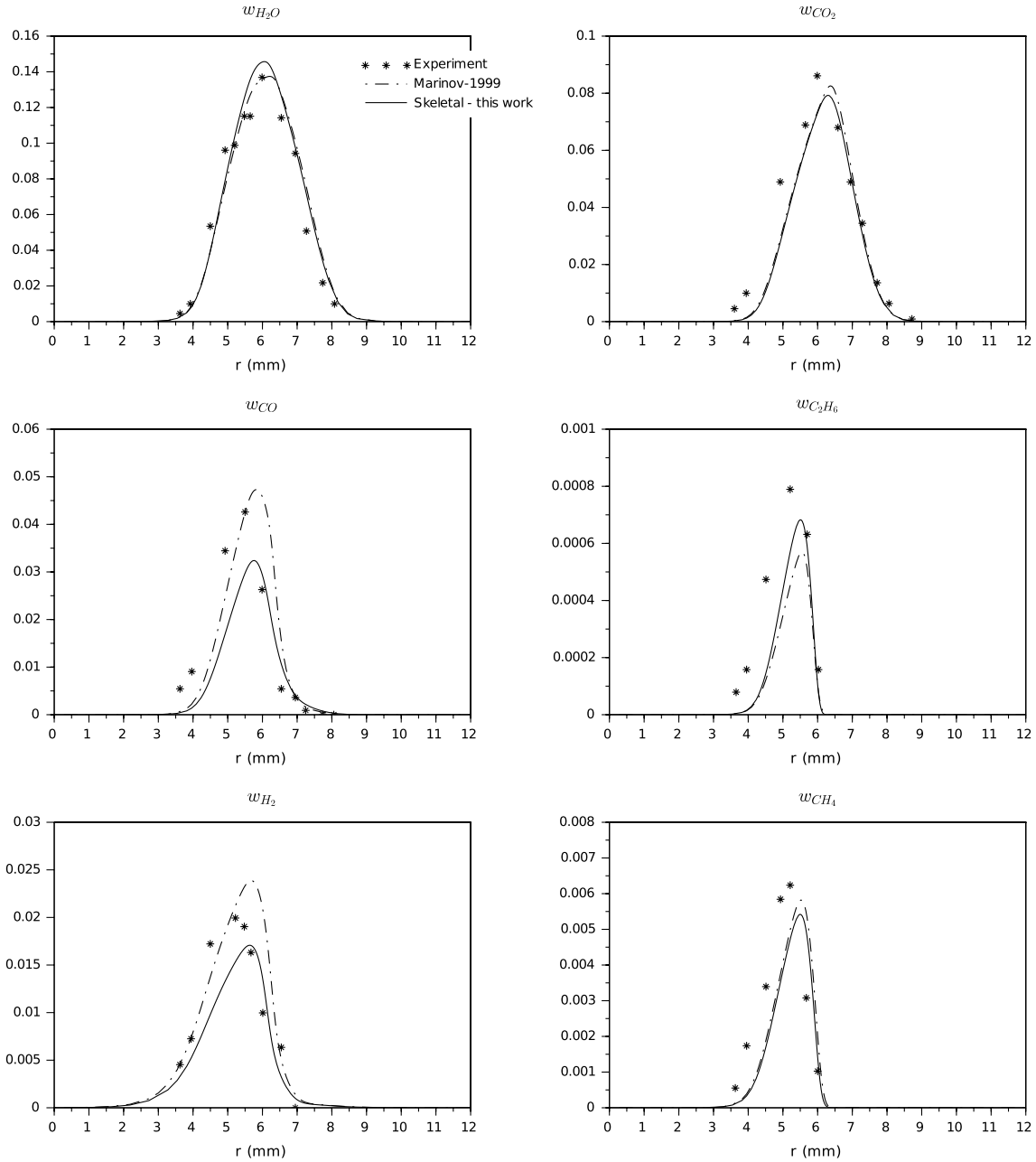

Fig. 12 Species mass fractions for skeletal and detailed for a non-premixed counterflow flame, compared with measurements [32]. The boundary conditions are given in Table 3

5 Conclusions

The purpose of this work was to present a different methodology for the mechanism reduction technique DRG and its implementation for ethanol. We show that a skeletal mechanism developed with the standard DRG with two applications (ignition delay time and flame speed) can reproduce other types of combustion processes for the ethanol oxidation.

Albeit the skeletal mechanism developed in this work does not take into account a counterflow and burner stabilized flames, it can be seen by the results that it reproduces these configurations. This is an important characteristic since, when dealing with high chain hydrocarbons or alcohols molecules, in which detailed mechanism can have thousand of elementary reactions and species, is possible to have a less effort to produce a skeletal mechanism that can reproduce a more demanding simulation. This also

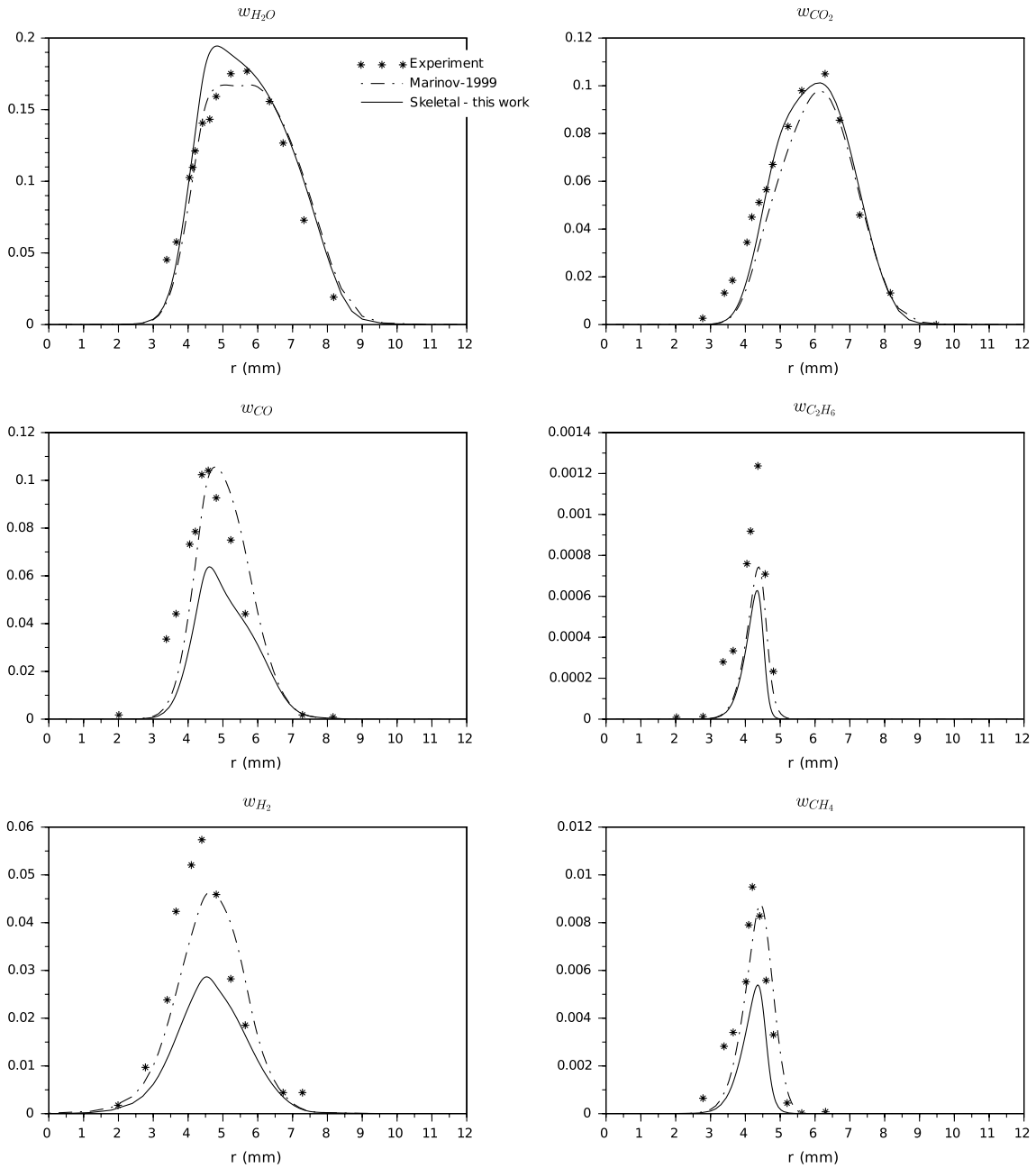

Fig. 13 Species mass fractions for skeletal and detailed for a premixed counterflow flame, compared with measurements [32]. The boundary conditions are given in Table 3

can lead to a smaller result in the number of species and reactions that are retained.

One question that arrives is which type of applications (and range of parameters) should be chosen when developing a skeletal mechanism with DRG, if one aims to reproduce more complex problems, e.g. turbulent flames? And which would be the minimum dimension that the reduced model should have—and how much the choice of applications can influence that—to reproduce other problems? These questions will be addressed in future works.

Acknowledgements Minuzzi thanks the financial support from Brazilian agency CAPES, under the grant N° 88881.132868/2016-01, and CNPq, under the process N° 140327/2018-5. We kindly acknowledge Philippe Dagaut from CNRS-INSIS for providing the experimental data.

References

1. An H, Yang W, Maghbouli A, Li J, Chua K (2014) A skeletal mechanism for biodiesel blend surrogates combustion. Energy Convers Manag 81:51–59
2. Chen Y, Chen JY (2018) Towards improved automatic chemical kinetic model reduction regarding ignition delays and flame speeds. Combust Flame 190:293–301
3. Co P (2018) British Petroleum Company. BP statistical review of world energy, June/2018
4. Curran HJ, Dunphy MP, Simmie JM, Westbrook CK, Pitz WJ (1992) Shock tube ignition of ethanol, isobutene and MTBE: experiments and modeling. In: Symposium (international) on combustion, vol 24. Elsevier, pp 769–776
5. Dias V, Katshiatshia HM, Jeanmart H (2014) The influence of ethanol addition on a rich premixed benzene flame at low pressure. Combust Flame 161(9):2297–2304
6. Dunphy MP, Patterson PM, Simmie JM (1991) High-temperature oxidation of ethanol. Part 2. Kinetic modelling. J Chem Soc Faraday Trans 87(16):2549–2559
7. Dunphy MP, Simmie JM (1991) High-temperature oxidation of ethanol. Part 1. Ignition delays in shock waves. J Chem Soc Faraday Trans 87(11):1691–1696
8. Egolfopoulos F, Du D, Law C (1992) A study on ethanol oxidation kinetics in laminar premixed flames, flow reactors, and shock tubes. In: Symposium (international) on combustion, vol 24. Elsevier, pp 833–841
9. Galassi RM, Ciottoli PP, Sarathy SM, Im HG, Paolucci S, Valorani M (2018) Automated chemical kinetic mechanism simplification with minimal user expertise. Combust Flame 197:439–448
10. Goodwin DG, Moffat HK, Speth RL (2017) CANTERA: An object-oriented software toolkit for chemical kinetics, thermodynamics, and transport processes. Version 2.3.0. http://www.cantera.org. Accessed 23 Feb 2018
11. Goussis DA, Maas U (2011) Model reduction for combustion chemistry. In: Echekki T, Mastorakos E (eds) Turbulent combustion modeling. Springer, Berlin, pp 193–220
12. Griffiths J (1995) Reduced kinetic models and their application to practical combustion systems. Prog Energy Combust Sci 21(1):25–107
13. Leplat N, Dagaut P, Togbé C, Vandooren J (2011) Numerical and experimental study of ethanol combustion and oxidation in laminar premixed flames and in jet-stirred reactor. Combust Flame 158(4):705–725
14. Liu W, Kelley AP, Law CK (2011) Non-premixed ignition, laminar flame propagation, and mechanism reduction of n-butanol, isobutanol, and methyl butanoate. Proc Combust Inst 33(1):995–1002
15. Løvås T (2012) Model reduction techniques for chemical mechanisms. INTECH Open Access Publisher, London
16. Lu T, Law CK (2005) A directed relation graph method for mechanism reduction. Proc Combust Inst 30(1):1333–1341
17. Lu T, Law CK (2006) Linear time reduction of large kinetic mechanisms with directed relation graph: n-heptane and iso-octane. Combust Flame 144(1):24–36
18. Lu T, Law CK (2006) On the applicability of directed relation graphs to the reduction of reaction mechanisms. Combust Flame 146(3):472–483
19. Luo Z, Plomer M, Lu T, Som S, Longman DE, Sarathy SM, Pitz WJ (2012) A reduced mechanism for biodiesel surrogates for compression ignition engine applications. Fuel 99:143–153
20. Marinov NM (1999) A detailed chemical kinetic model for high temperature ethanol oxidation. Int J Chem Kinet 3(2):257–263
21. Metcalfe WK, Burke SM, Ahmed SS, Curran HJ (2013) A hierarchical and comparative kinetic modeling study of c1–c2 hydrocarbon and oxygenated fuels. Int J Chem Kinet 45(10):638–675
22. Millán-Merino A, Fernández-Tarrazo E, Sánchez-Sanz M, Williams FA (2018) A multipurpose reduced mechanism for ethanol combustion. Combust Flame 193:112–122
23. Mittal G, Burke SM, Davies VA, Parajuli B, Metcalfe WK, Curran HJ (2014) Autoignition of ethanol in a rapid compression machine. Combust Flame 161(5):1164–1171
24. Ng HK, Gan S, Ng JH, Pang KM (2013) Development and validation of a reduced combined biodiesel–diesel reaction mechanism. Fuel 104:620–634
25. Niemeyer KE, Sung C (2011) On the importance of graph search algorithms for DRGEP-based mechanism reduction methods. Combust Flame 158(1):1439–1443
26. Niemeyer KE, Sung C, Raju MP (2010) Skeletal mechanism generation for surrogate fuels using directed relation graph with error propagation and sensitivity analysis. Combust Flame 157(1):1760–1770
27. Okuyama M, Hirano S, Ogami Y, Nakamura H, Ju Y, Kobayashi H (2010) Development of an ethanol reduced kinetic mechanism based on the quasi-steady state assumption and feasibility evaluation for multi-dimensional flame analysis. J Therm Sci Technol 5(2):189–199
28. Olm C, Varga T, Valkó É, Hartl S, Hasse C, Turányi T (2016) Development of an ethanol combustion mechanism based on a hierarchical optimization approach. Int J Chem Kinet 48(8):423–441
29. Pepiot-Desjardins P, Pitsch H (2008) An efficient error-propagation-based reduction method for large chemical kinetic mechanisms. Combust Flame 154(1):67–81
30. Poinsot T, Veynante D (2011) Theoretical and numerical combustion, 3rd edn. RT Edwards, Inc., Murarrie
31. Röhl O, Peters N (2009) A reduced mechanism for ethanol oxidation. In: 4th European combustion meeting (ECM 2009). Austria, April, Vienna, pp 14–17
32. Saxena P, Williams FA (2007) Numerical and experimental studies of ethanol flames. Proc Combust Inst 31(1):1149–1156
33. Seshadri K, Lu T, Herbinet O, Humer S, Niemann U, Pitz WJ, Seiser R, Law CK (2009) Experimental and kinetic modeling study of extinction and ignition of methyl decanoate in laminar non-premixed flows. Proc Combust Inst 32(1):1067–1074
34. Tomlin AS, Turányi T, Pilling MJ (1997) Mathematical tools for the construction, investigation and reduction of combustion mechanisms. Compr Chem Kinet 35:293–437
35. Tosatto L, Bennett BAV, Smooke MD (2013) Comparison of different drg-based methods for the skeletal reduction of jp-8 surrogate mechanisms. Combust Flame 160(9):1572–1582
36. Turanyi T, Berces T, Vajda S (1989) Reaction rate analysis of complex kinetic systems. Int J Chem Kinet 21(2):83–99
37. Turányi T, Tomlin AS (2014) Analysis of kinetic reaction mechanisms. Springer, Berlin
38. UCSD (2014) Chemical-kinetic mechanisms for combustion applications, San Diego mechanism web page, Mechanical and aerospace engineering (combustion research), University of California at San Diego, Version 2014-10-04. http://combustion.ucsd.edu. Accessed 20 May 2018
39. Wang X, Liu H, Zheng Z, Yao M (2015) A skeletal mechanism of a biodiesel surrogate fuel for compression ignition engines. Energy Fuels 29(2):1160–1171
40. Yu C, Minuzzi F, Bykov V, Maas U (2019) Methane/air autoignition based on global quasi-linearization (GQL) and directed relation graph (DRG): implementation and comparison. Combust Sci Technol 12:1–23